

# Reducing boundary effects in a kernel-based classifier

PENG GONG

Department of Geomatics Engineering, The University of Calgary, Calgary,  
Alberta, Canada T2N 1N4

(Received 1 August 1993; in final form 4 November 1993)

**Abstract.** In this letter, a method is presented to reduce misclassification at the boundaries between different types of land covers. Errors are caused by use of spatial features extracted from pixel neighbourhoods. Simple thresholding and region-growing techniques are used to reduce such errors. The method is included as an extension to a frequency-based contextual classifier (FBC).

Some experiments have been carried out to evaluate both the original classifier, FBC, and the extended version using an image acquired with a Compact Airborne Spectrographic Imager (CASI). Experimental results show that overall classification accuracies with the CASI image are 84·80 per cent and 89·37 per cent obtained using the FBC and the extended FBC, respectively.

## 1. Introduction

A major barrier to improving classification accuracies in image classification involving spatial features extracted from local neighbourhoods (pixel windows) is the lack of methods in reducing the misclassification that occurs at boundaries of different classes. This type of misclassification, referred here as boundary effects, is caused by the use of pixel neighbourhoods (e.g., Gong and Howarth 1992 a, b). An example illustrating this phenomenon is found in Eyton (1993) where a frequency-based classification algorithm is used to classify urban land uses from digitized aerial colour photographs.

A frequency-based contextual classifier (FBC) involves the use of frequency tables extracted from pixel neighbourhoods in classification (Eyton 1993, Barnsley and Barr 1993, Gong and Howarth 1992 a, b, Zhang *et al.* 1988, Wharton 1982). In this method the multispectral image to be classified is first transformed into a single-channel image. This is usually achieved by classifying the image into more detailed land-cover classes, which are related to the final classification task, using clustering or supervised classification methods. The frequency-based classifier is then applied to the transformed image with a pixel-window of a specific size to generate a classification map. To speed up the transformation, gray-level vector reduction can be used (Gong and Howarth 1992 b).

Eyton (1993) has made the first effort to reduce boundary effects in an FBC. After a land-use map was obtained from the FBC, it was found that instead of 8 defined land-cover classes 17 classes were produced. An inspection was made to identify the real land-use classes corresponding to 'core regions', from those classes affected by the boundary effect corresponding to 'boundary regions'. A relabelling procedure was used to convert those boundary regions to the core regions from which their pairwise squared generalized distances were the shortest (Eyton 1993). Such a treatment has two drawbacks. The first is that visual inspection is subjective

and time-consuming when the boundary classes are not clearly observable. As will be shown in section 3, the second is that converting an entire boundary class to only one core class may be biased because each boundary class is usually composed of two or more core classes.

In this letter, an alternate boundary-effect reduction method is presented. Although it is developed as an extension to the specific frequency-based contextual classifier reported in Gong and Howarth (1992b), the procedure is generally applicable.

## 2. Boundary effects and their reduction

### 2.1. Boundary effects

The boundary effect can be illustrated using a simple example. In figure 1 there presumably exist only two land-use classes: Classes A and B. As a pixel window moves from the area of Class A across the boundary to the area of Class B, the occurrence frequencies extracted from each move of the pixel window change. Assume Class A is industrial/commercial with concrete surface dominant and Class B is golf course with grass dominant. If a pixel window moves from Class A to Class B, one will observe that frequencies extracted from this window change from concrete surface dominating, to similar proportions of concrete surface and grass, to high grass proportion and low concrete proportion, and finally to grass dominating the pixel window. The central two concrete and grass configurations are transitional from Class A to Class B, and depending on other classes included in the classification scheme their frequencies may be more similar to new residential or old residential classes. Thus, as a pixel window moves across the boundary between two classes, four or even more land-use classes would be obtained; those transitional classes are errors.

The level of boundary effects changes as the configuration of image resolution and class definition changes. For a given class, the size and shape of ground components affect the level of boundary effects. If those ground components are important features for discriminating the specific class from others. The image resolution needs to be sufficiently fine to allow those components to be observable on the image. The pixel window needs to be large enough to allow those components to be covered in one pixel window in order to guarantee that frequencies extracted are representative to the class. Generally, boundary effects tend to be more serious

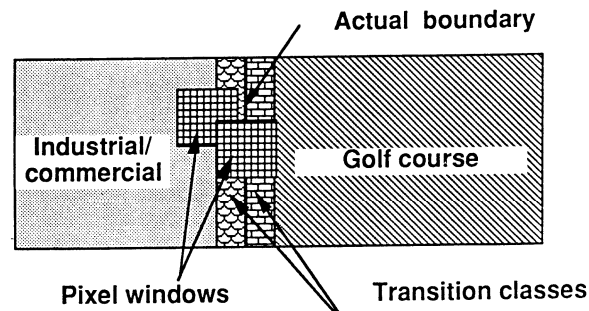


Figure 1. An illustration of the pixel-window effect on the classification results at the boundary of two distinct land-use classes. The two patterns between A and B are the transitional classes which are misclassified by an FBC.

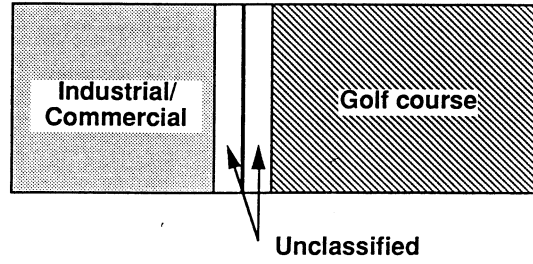


Figure 2. An illustration of the thresholding and region-growing procedures. The thresholding prevents the area along the boundary of two classes from being classified. The region-growing algorithm will then be used to fill up the gap between classes A and B.

as image spatial resolution decreases because coarser resolution will smooth out the boundary effects. On the other hand, boundary effects will increase as the size of pixel window increases.

### 2.2. Threshold controlled classification

Since the boundary effect is a spatial problem, it should be corrected spatially. In the FBC (Gong and Howarth, 1992 b), a city-block distance  $d_s(i,j)$  is calculated as a basis for classification:

$$d_s(i,j) = \sum_{k=1}^n \left| f_k(i,j) - c_{sk} \right|$$

where  $f_k(i,j)$  is the extracted frequency of grey-level vector  $k$  from a pixel window centered around pixel location  $(i,j)$ .  $C_s = \{c_{s1}, c_{s2}, \dots, c_{sn}\}^T$  is the average gray-level vector frequency for a land-use class  $s$ ;  $C_s$  can be obtained from supervised training on the gray-level vector-reduced image. The pixel window size is  $m \times m$ .  $n$  is the total number of grey-level vectors.

Instead of directly comparing the shortest distance among all the land-use classes, once  $d_s(i,j)$  is obtained, it is compared with a threshold  $\beta \cdot m^2$  ( $0 < \beta < 2$ ). If  $d_s(i,j) \leq \beta \cdot m^2$ , pixel  $(i,j)$  is a candidate for land-use class  $s$ . Otherwise, pixel  $(i,j)$  is rejected from land-use class  $s$ . If more than one land use class is a candidate, pixel  $(i,j)$  belongs to the closest land-use class.  $\beta=2$  is equivalent to applying no thresholding whereas  $\beta=0$  implies that only those pixels whose calculated occurrence frequencies match exactly with those of a particular class will be classified. Therefore, by adjusting the threshold  $\beta$  between 0 and 2 some transitional classes between boundaries of two different classes may remain unclassified.

### 2.3. Region growing by majority filtering

A simple region-growing procedure can then be applied iteratively to fill up the gaps (unclassified pixels) between two classes (figure 2). In this procedure, only unclassified pixels may be affected. An unclassified pixel is first located. Its eight neighbours is then checked to see if any of these neighbours has been classified. If the answer is no, the algorithm searches for the next unclassified pixel and does the same neighbourhood check. If the answer is yes, the majority rule is applied to label the unclassified pixel. The number of unclassified pixels is usually small (less than 10

per cent in an image). In addition, the region-growing procedure is computationally simple. Therefore, it requires a very small amount of computation.

The iterating region-growing procedure is terminated according to either (1) a user determined number of iteration or (2) when every unclassified pixel is assigned a class. If a classification scheme is not complete for an area, there should be pixels remaining unclassified at the end of a classification task. In this case, one should use the number of iterations as the criterion to control the region-growing procedure. A suggested number of iterations is  $m/2 + 1$  (i.e., the lateral length of the pixel-window used). This is because the maximum width of any unclassified gaps is  $m$ , and in each iteration the algorithm fills up a two-pixel wide gap. On the other hand, if the classification scheme is perfectly suitable for an area, the region growing could be terminated when all pixels are classified. In this study, the second criterion is selected.

### 3. Experimental design

#### 3.1. Data and classification scheme

With a compact airborne spectrographic imager (CASI), an image was acquired on 6 September 1991 over the west side of the City of Calgary, Alberta, Canada. CASI is an imaging spectrometer for use on board small aircraft or in laboratories (Anger *et al.* 1990). This image has a spatial resolution of approximately 7.5 m by 7.5 m with 512 by 512 pixels. Its 8 spectral bands cover 449.0–507.5 nm, 509.3–571.6 nm, 573.4–610.9 nm, 652.1–689.8 nm, 733.1–769.2 nm, 771.0–807.1 nm, 809.0–850.6 nm, and 852.5–899.7 nm, respectively. A false colour composite of bands 3, 4, and 8 is shown in figure 3. No radiometric correction was made to the image because it does not offer much help for a relatively small and flat area (Landgrebe and Malaret 1986).

The study site includes the Glenmore Reservoir and is surrounded primarily by residential and recreational land-use types. A land-use classification scheme of seven classes was used (table 1). The residential area was broken into two classes: old and new residential area, with the old residential area having a greater amount of landscaping and vegetation. The recreational land-cover class mainly refers to the golf course at the north side of the reservoir.

#### 3.2. Classification

The frequency-based contextual classifier is coded as a module of PCI's EASI/PACE image analysis package which can be run on any platform PCI supports. Source code is available from the author.

Table 1. Land-use classification scheme.

Land-Use Class	Code	Colour
Old Urban Residential	RES1	Red
New Urban Residential	RES2	Green
Industrial/Commercial	IND/COM	Blue
Water	WATER	Yellow
Recreational	REC	Magenta
Grassland	GRASS	Cyan
Forest	FOR	White



Figure 3. The false colour composite of the CASI image used in this study. Bands 3, 4 and 8 have been displayed using blue, green and red colour guns.



Figure 4. The classification results obtained using the frequency-based contextual classifier with a pixel-window size of  $13 \times 13$ .

As in conventional supervised classification, blocks of pixels were selected for class signature generation. Test samples were selected in the same manner as in the training sample selection. For each land-cover class, a few blocks of pixels with certain proportion of pixels close to land-cover boundaries were selected. To avoid over-estimation of classification accuracies, care has been taken to make sure that test samples do not overlap with training samples.

Two factors affect the generation of gray-level vector-reduced images: the covariance matrix used to construct the eigen space, and the specified number of output gray-level vectors. The covariance matrix can be calculated from the entire image, any specific part of the image, or the training samples. A suggestion is to use training samples if the size of training samples is large enough. This is because statistics generated from appropriately selected training samples would usually enhance the separabilities among the land-use classes, and thus it is more likely that a gray-level vector-reduced image with a greater discriminating power would be generated. The number of gray-level vectors specified for the output image also affects the discriminating power of the output image. While too few gray-level vectors would definitely lead to loss of discriminating information, there seems to be an upper limit for the number of gray-level vectors beyond which little classification-accuracy improvement can be achieved. In this study training samples were used to calculate the covariance matrix, and a gray-level vector-reduced image with 50 gray-level vectors was generated. All the eight bands of the original CASI image were used to produce the gray-level vector-reduced image. A detailed description on determining possible optimal number of grey-level vectors can be found in Gong and Howarth (1992 b).

Pixel window sizes ranging from  $7 \times 7$  to  $17 \times 17$  were tested by applying the FBC and the extended FBC to the grey-level vector-reduced image. For the extended FBC, thresholds of 0.7, 0.8, 0.9, 1.0, 1.1, and 1.2 were tested.

#### 4. Results

The classification results obtained from the FBC with a pixel-window size of  $13 \times 13$  is shown in figure 4 which represents the best overall classification results among all the window sizes used. Figure 5 shows the intermediate classification results obtained with the extended FBC with a pixel-window size of  $13 \times 13$  and a threshold value of 0.8. It can be seen from figure 5 that at most parts of the boundaries between two land-cover classes, gaps with varying widths have been produced. The final results of the extended FBC are shown in figure 6 that is obtained from the intermediate results (figure 5) with the region-growing algorithm.

Tables 2 and 3 show the confusion matrices, the producer's and user's accuracies (Story and Congalton 1986) for the classifications obtained with the FBC and the extended FBC, respectively. The class entries in the first row serve as the reference while those entries in the first column represent the classification results. The overall classification accuracies with the FBC and the extended FBC are 84.80 per cent and 89.37 per cent, respectively. The overall accuracy improvement from the original FBC to the extended FBC is 4.57 per cent which primarily resulted from the relatively large accuracy improvement for the grass class. It can be seen that areas of the misclassified class of residential 1 located at the boundary between the grass and the water classes have been removed or partly reduced in size on figure 6 as compared with figure 4.

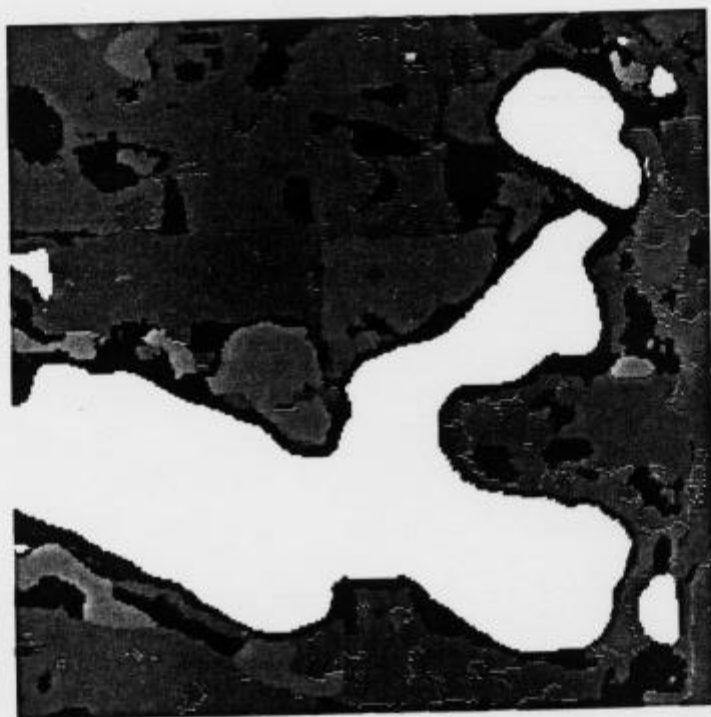


Figure 5. The intermediate classification results obtained using the extended frequency-based contextual classifier with a pixel-window size of  $13 \times 13$  and a threshold of 0.8.



Figure 6. The final classification results obtained with the extended frequency-based contextual classifier after region growing being applied.

Table 2. Confusion matrix derived from the frequency-based contextual classification with a pixel-window size of  $13 \times 13$ .

Classified results	Reference							User's %
	Res 1	Res 2	Ind/Comm	Water	Rec	Grass	For	
Residential 1	1189	9	102		101	188	265	64.13
Residential 2	82	704	64		11	190		66.98
Ind/Comm			326					100.00
Water				1401				100.00
Recreational					967			100.00
Grassland						698		100.00
Forest							362	100.00
$\Sigma$ Column	1271	713	492	1401	1079	1076	627	
Producer's %	93.55	98.74	66.26	100.00	89.62	64.87	57.74	
Overall %	84.80							

## 5. Conclusions

Thresholding and region-growing procedures have been added to the frequency-based contextual classifier (FBC) (Gong and Howarth 1992 b). The extension requires a relatively small amount of computation. Test has been carried out with a Compact Airborne Spectrographic Imager (CASI) image of 8 spectral bands ranging from the visible to near-infrared with a spatial resolution of approximately  $7.5 \text{ m} \times 7.5 \text{ m}$ . Results indicate that the FBC and its extended version both produced overall classification accuracies of greater than 80 per cent. When used to classify

Table 3. Confusion matrix derived from the extended frequency-based contextual classification with a pixel-window size of  $13 \times 13$  and a threshold of 0.8.

Classified	Reference							User's %
	Res 1	Res 2	Ind/Comm	Water	Rec	Grass	For	
Residential 1	1189	8	132		100	26	243	70.02
Residential 2	82	705	67		15	35		77.99
Ind/Comm			293					100.00
Water				1401				100.00
Recreational					964			100.00
Grassland						1015		100.00
Forest							384	100.00
$\Sigma$ Column	1271	713	492	1401	1079	1076	627	
Producer's %	93.55	98.88	59.55	100.00	89.34	94.33	61.24	
Overall %	89.37							



rural-urban fringe areas the FBC algorithm works very well with the airborne CASI image. Through boundary effect reduction, it is possible to further improve classification accuracies obtained with the FBC.

It may be possible to apply the boundary effect reduction method in other types of contextual classification algorithms such as those employing textual features. This may be achieved by adding a threshold component in the classifier to isolate transitional classes and using the region-growing method to replace the isolated classes with more appropriate classes.

### Acknowledgments

This research was partially supported by an NSERC Research Grant to P. Gong. The CASI image was provided by Itres Instruments of Calgary. The three anonymous reviewers helped to improve the clarity of this letter.

### References

- ANGER, C. D., BABEY, S. K., and ADAMSON, R. J., 1990. A New Approach to Imaging Spectrometry, *Proceedings of Society of Photo-optical Instrumentation Engineers* (Orlando, Florida: SPIE), **1298**, 72-86.
- BARNSELY, M. J., and BARR, S. L., 1992. Developing spatial re-classification techniques for improved land-use monitoring using high spatial resolution images. *Archives of the 17th Congress of International Society of Photogrammetry and Remote Sensing*, Washington, D.C., 8-14 August 1992, Vol. VII (Washington, DC: ISPRS), pp. 646-654.
- EYTON, J. R., 1993. Urban land use classification and modelling using cover-type frequencies. *Applied Geography*, **13**, 111-121.
- GONG, P., and HOWARTH, P. J., 1992 a. Land-use classification of SPOT HRV data using a cover-frequency method. *International Journal of Remote Sensing*, **13**, 1459-1471.
- GONG, P., and HOWARTH, P. J., 1992 b. Frequency-based contextual classification and gray-level vector reduction for land-use identification. *Photogrammetric Engineering and Remote Sensing*, **58**, 423-437.
- LANDGREBE, D. A., and MALARET, E., 1986. Noise in remote sensing systems: the effects on classification error. *I.E.E.E. Transactions on Geoscience and Remote Sensing*, **24**, 294-300.
- STORY, M., and CONGALTON, R. G., 1986. Accuracy assessment, a user's perspective. *Photogrammetric Engineering and Remote Sensing*, **52**, 397-399.
- WHARTON, S. W., 1982. A contextual classification method for recognizing land use patterns in high resolution remotely sensed data. *Pattern Recognition*, **15**, 317-324.
- ZHANG, Z., SHIMODA, H., FUKUE, K., and SAKATA, T., 1988. A new spatial classification algorithm for high ground resolution images. *Proceedings of IGARSS'88 held at Edinburgh, U.K., 12-18 September, 1988* (New York: The I.E.E.E. Inc.) pp. 509-512.